Expression and purification of recombinant wheat translation initiation factor eIF2

Shinetin Tzeng

In partial fulfillment of the requirements for graduation with the Dean's Scholars Honor's Degree in the School of Biological Sciences

_____ _____

Supervising Professor Date

Abstract

Proteins carry out the activities for cellular growth and maintenance in a timely and space-specific manner, so the formation of proteins from their genetic counterparts, or translation, must be tightly controlled. Regulation occurs primarily during the initiation step of translation, a highly involved process that properly positions messenger RNA, methionine-charged initiator transfer RNA, and ribosomes via a family of proteins known as eukaryotic initiation factors (eIFs). One of these proteins is eIF2, a trimeric complex made of eIF2α, eIF2β, and eIF2γ. In mammalian and yeast systems, the phosphorylation of eIF2α by specific kinases and its downstream effects down-regulate global protein synthesis, and the mechanism has been widely studied. However, in plants, evidence suggests that different regulatory pathways may be involved. To ultimately describe the molecular and biochemical basis by which higher plants regulate protein synthesis, studies of mutant eIF2α and the effects of phosphorylation are necessary. To achieve this goal, genes for the three subunits of wheat eIF2 were synthesized *de novo* by overlapping oligonucleotides that were optimized for *E. coli* codon usage, and then the genes were cloned into an operon for expression of the complex in *E. coli*. This particular study focuses on optimizing the conditions for expression and purification of soluble eIF2 complexes. Alterations in the strain of *E. coli*, growth condition and media, and operon construct were tested to enhance eIF2 expression and solubility, and different methods of purification were applied. However, at this point, the expression and purification of eIF2 still remains unsuccessful.

Background

Translational Control

Proteins take on enzymatic, structural, regulatory, and transport roles for the day-to-day functioning of living cells. Up to 40% of the total energy requirements of a cell and a large part of its resources are spent in the synthesis of these macromolecules, a process also known as translation (Buttgereit and Brand 1995). This process of decoding messenger RNA into a chain of amino acids occurs in 3 distinct multi-step phases—initiation, elongation, and termination.

Translational initiation is the rate-limiting or slowest of the three phases. In experiments where cells were treated with low concentrations of cycloheximide, an elongation inhibitor, total protein synthesis was only reduced by 5%, an amount that would be higher if elongation were the limiting phase (Walden et al. 1981). Rates of initiation were quantified by dividing the polysome size (number of active ribosomes on a mRNA) by the ribosome transit time (time it takes for the ribosome to travel from start to end of the mRNA), and rates of elongation were measured by dividing the number of amino acids incorporated in the protein by the ribosome transit time. When calculated, the numbers were different for each specific mRNA, but generally, initiation rates were significantly slower than elongation rates. Because it is the rate-limiting phase of translation, many translational regulatory mechanisms are found in initiation.

Translational controls explain why cellular protein levels do not correspond one-to-one with cellular mRNA levels. Given the large resource and energy expenditure involved in protein synthesis, it is sensible for regulatory mechanisms to exist at the beginning of the process so that the cell doesn't waste its limited supply of materials and

energy. However, if the early placement in the pathway was the only reason for regulation at this phase, then it would make more sense for transcription, which occurs before translation in the pathway of gene expression, to be the major target of control. So why then do cells utilize mechanisms of translational control? For some systems, like reticulocytes that have no nucleus and early-stage embryos that experience no transcription from the zygotic nucleus, translational control is the only way to regulate the proteome and thus must be sufficient for regulation of gene expression. For systems that utilize both transcriptional and translation control, the latter has come to dominate because it confers specific advantages. For example, a cell regulating its translation levels can immediately implement changes in response to intracellular and extracellular stimuli; as opposed to the splicing and nuclear transport events that occur post-transcriptionally, there are no major biochemical reactions downstream of translation that could potentially delay the response. In addition, translational control is easily reversible because regulation occurs largely via the phosphorylation of the components of the translational machinery, as will be discussed in later sections. Lastly, while transcriptional control mainly focuses on the regulation of individual genes or classes of genes, translational control is more powerful for its broad effects, affecting nearly the entire cellular transcriptome. However, this does not exclude the possibility of fine-tuning protein levels in space and time through mRNA-specific translational control. Polarized cells, like oocytes and early embryos, often rely on mRNA-specific mechanisms to ensure that protein synthesis occurs only at specific locations of the cell so that protein morphogen gradients are properly set up in the cell for anterior to posterior axis formation (Gebauer and Hentze 2004). Translational control of specific mRNAs in

time can be seen following amino acid depletion in cells, where mRNAs of specific transcription factors are highly translated into proteins that can then activate genes involved in metabolism and transport of amino acids or apoptosis (Wek et al. 2006). Clearly, regulated protein levels via translational controls are essential not only for the normal everyday operations of cells but also vital for quick, reversible, effective adaptations to new stimuli or stresses.

Mechanism of Translation Initiation

We must understand the events of translation initiation and identify the key players of each step to appreciate the different levels of control. Studies of the mechanism in yeasts and mammals are widely documented, so we will focus on eukaryotic translation initiation. For the most part, the mechanism is conserved in higher eukaryotes, and the ultimate goal of translation initiation is to assemble the 80S ribosome and methionine-charged initiator tRNA carrying the CAU anticodon at the initiation AUG codon of mRNA. This occurs through multiple steps with the active involvement of multiple proteins known as eukaryotic initiation factors (eIFs). The important steps of translation initiation and the promoting players of each step follow and are diagrammed in **Figure 1.**

The 80S ribosome dissociates into its 60S and 40S subunits, and the latter is stabilized by eIF3, eIF1A, and eIF1. The interaction of these 3 eIFs with the 40S ribosomal subunit is not sufficient for maintaining the separation of the ribosomal subunits and eIF2 found in a ternary complex is also a necessary cofactor. The formation of this ternary complex, consisting of eIF2, GTP, and Met-tRNA$_i^{Met}$, is actually the first step in translation initiation. eIF2 is usually in association with GDP and cannot bind

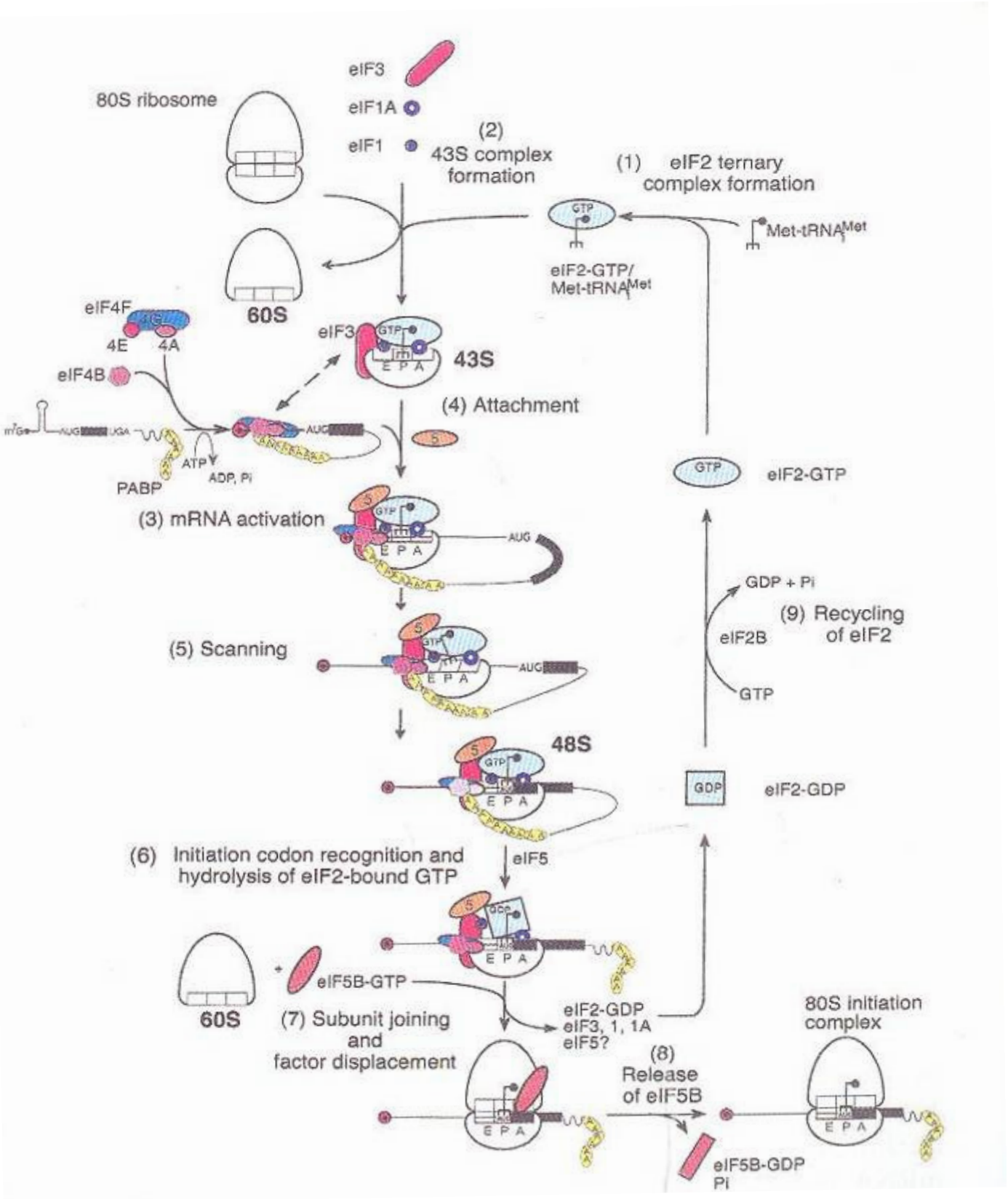

Figure 1. Mechanism of eukaryotic translation initiation (Pestova et al. 2007).

exchange the GDP for GTP, an event that increases the affinity of eIF2 for the methionine moiety of Met-$tRNA_i^{Met}$ so the ternary complex can form (Kapp and Lorsch 2004). Detailed information about eIF2 will be provided in the next section as this eIF is the focus of this study. When the ternary complex binds to the P site of the 40S ribosomal subunit already associated with eIF3, eIF1A, and eIF1, the 43S preinitiation complex is formed and ready to bind mRNA, a step mediated by a new set of eIFs.

All mRNAs coming from the nucleus go through post-transcriptional modification, including the addition of a 5' 7-methylguanosine cap and 3' poly-A tail. These two mRNA elements are bound by eIF4E and poly(A)-binding protein (PABP), respectively, which are found in association with eIF4G, a large scaffold protein. These protein interactions circularize and stabilize the mRNA. eIF4G also binds eIF3, bringing the mRNA to the 43S preinitiation complex. To enhance this latter interaction, eIF4A, an ATPase with helicase activity, binds to eIF4G, and when activated by eIF4B and eIF4H, eIF4A unwinds any secondary structure in the 5' untranslated region of the mRNA.

Next, the 43S preinitiation complex in an "open" conformation scans the mRNA in an ATP-independent fashion until it finds the first AUG triplet, which is recognized by complementary base-pairing with the tRNA anticodon. Support for the scanning model comes from inserting an AUG triplet 5' of the original start codon and seeing that the complex will assemble at the newly inserted site. Though not essential for the scanning ability of the 43S complex, the eIF4 class of proteins usually remains associated to ensure the ribosome's processivity by unwinding any internal secondary structure of mRNA. When there is correct base-pairing of tRNA anticodon and mRNA codon, the ribosomal complex stalls and forms the 48S initiation complex in a "closed" conformation on the

start codon. eIF1 ensures the fidelity of initiation by dissociating any aberrantly formed 48S complexes. In mammalian and yeast systems, start codon selection is slightly more complicated as the -3 and +4 nucleotide positions must be occupied by A/G and G, respectively, for optimal translation initiation at the specific AUG codon (Kozak 1991). These context nucleotides interact with specific sites on eIF2 and 18S rRNA of the preinitiation complex and provide an additional check on fidelity (Pisarev et al. 2006).

For translation initiation to be complete, the eIFs must be displaced so that the 60S ribosomal subunit can rejoin the 40S ribosomal subunit now associated with mRNA and tRNA. This requires eIF5, an eIF2-specific GTPase-activating protein (GAP), and eIF5B, a ribosome-dependent GTPase. eIF5 activation depends on stable formation of the 48S initiation complex, and when activated, eIF5 induces the hydrolysis of the GTP bound to eIF2, so that eIF2 has an lower affinity for Met-tRNA$_i^{Met}$ as well as weaker interaction with the 40S ribosomal subunit. However, this event does not immediately displace eIF2-GDP and the other eIFs from the 40S ribosomal subunit because eIF2 makes a direct interaction with the -3 nucleotide on the mRNA and the other eIFs are stabilized by the presence of mRNA on the 40S subunit (Pisarev et al. 2006, Unbehaun et al. 2004). The displacement of all eIFs is mediated by the contact of eIF5B and the 60S ribosomal subunit to the 48S complex. The hydrolysis of the GTP bound to eIF5B is actually not required for the displacement of the rest of the eIFs but is required to remove eIF5B itself from the A site of the 80S ribosome, so that a charged tRNA corresponding to the second codon of the mRNA can enter the ribosome, and translation elongation can proceed.

There are still many details of translation initiation to be resolved, but hopefully the complexity of translation initiation can be appreciated by this overview of the process. When any of the steps or proteins involved in each step are altered, translation is affected and cells may be thrown out of homeostasis. Cells may also alter any of these steps or proteins involved in each step to control intracellular protein synthesis levels to prevent getting thrown out of homeostasis.

eIF2 Structure and Function

From here on, we will focus on eIF2, a key player in the early steps of translation initiation, and how its regulation is achieved. eIF2 is a heterotrimer composed of a large γ subunit and smaller α and β subunits. eIF2 binds Met-tRNA$_i^{Met}$ in a GTP-dependent manner and facilitates the binding of Met-tRNA$_i^{Met}$ to the 40S ribosomal subunit. eIF2γ (mammalian, yeast, plant: 52kDa) has three domains: a GTP-binding domain (G domain), Domain II, and Domain III, where the latter two pack against the former to create a pocket where the 3' aminoacyl end of Met-tRNA$_i^{Met}$ binds (Alone et al. 2008). The G domain contains Switch I and Switch II elements marked by specific sequence motifs, and when GTP binds to the elements, they undergo structural rearrangements that affect Domains II and III and trigger the formation of the Met-tRNA$_i^{Met}$ pocket. eIF2γ has GTPase activity, and upon eIF5-activated hydrolysis of GTP to GDP and P_1 release, Switch I and II undergo structural rearrangements, such that the Met-tRNA$_i^{Met}$ pocket does not form, decreasing the affinity of the tRNA (Yatime et al. 2006). Because of its association with GTP and GDP, it makes sense that the G domain of eIF2γ has binding sites for eIF5 (GAP) and eIF2B (GEF) (Alone and Dever 2006).

Much less is known of eIF2β (mammalian, yeast, plant: 38kDa). The N-terminus contains lysine blocks that binds eIF5 and eIF2B (Asano et al. 1999), the middle region binds near eIF2γ's G domain, and the C-terminus with the zinc binding motif binds RNA and is involved in start codon selection (Donahue et al. 1988). The -3 nucleotide binds eIF2 to add another check on fidelity of correct codon-anticodon base-pairing. Initiation at UUG codons has been observed when the C-terminus of eIF2β is mutated.

eIF2α (mammalian, yeast: 36kDa, plant: 42kDa) functions mainly as the regulatory subunit of the heterotrimer as it is the target eIF2α kinases activated by cell stress, which is extensively discussed in the next section. It consists of two domains: a N-terminal domain with a nonspecific oligonucleotide (RNA) binding-fold and a C-terminal domain that binds the 40S ribosomal subunit and eIF2γ adjacent to the Met-tRNA$_i^{Met}$ pocket, stabilizing the bond between eIF2γ and Met-tRNA$_i^{Met}$ (Ito 2004, Yatime et al. 2004). See **Figure 2** for a general model for the proposed structure and interactions of the three subunits of eIF2. Notice that eIF2α and eIF2β don't directly bind each other.

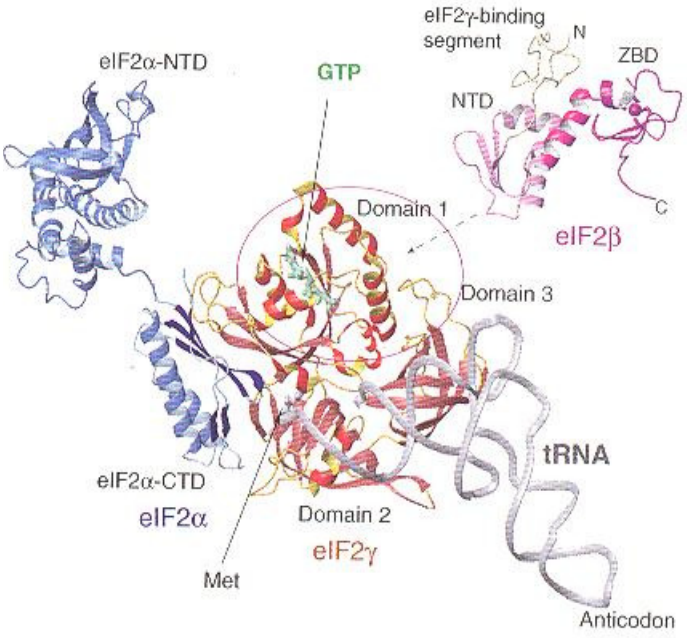

Figure 2. Structure of eIF2 in association with GTP and Met-tRNA$_i^{Met}$ to form ternary complex. eIF2α is shown in blue; eIF2β is shown in purple and beige; eIF2γ is shown in red. (Pestova et al. 2007).

Translational Control via eIF2α Phosphorylation

A major mechanism of translational control in mammalian and yeast systems is the reversible phosphorylation of eIF2α. When eIF2α is phosphorylated at Ser-51, there is a decrease in the general rate of protein synthesis. After a round of initiation, eIF2 is found in a complex with GDP and is unable to form the active ternary complex to participate in another round of initiation unless recharged by the exchange of GDP for GTP. eIF2B catalyzes this reaction where eIF2 is the substrate. However, when eIF2α is phosphorylated, eIF2(αP) has about a 150-fold higher affinity for eIF2B and becomes a competitive inhibitor of eIF2B (Rowlands et al. 1988). In all cells, amounts of eIF2B are limited relative to amounts of eIF2, and when all eIF2B is sequestrated in eIF2(αP)-eIF2B complexes, nucleotide exchange on eIF2 does not occur, most of the eIF2 becomes complexed with GDP, ternary complexes cannot form, and another round of initiation cannot occur.

There are four known eIF2α kinases (HRI, PKR, PERK, and GCN2) that all share a conserved eIF2α kinase domain. However, they each have a distinct regulatory domain that confers their ability to respond to different stimuli. Specifically, HRI is activated by low heme, heat shock, osmotic stress, nitric oxide, and certain toxins (Lu et al. 2001); PKR is activated by the presence of dsRNA from viral infection (Nanduri et al 2000); PERK is activated by ER stress due to the imbalance of unfolded proteins and chaperones (Bertolotti et al 2000); and GCN2 is activated by uncharged tRNA from amino acid starvation (Hinnebusch 2005). Despite the different upstream activators, all of the eIF2α kinases have the downstream effect of phosphorylating eIF2α and attenuating the initiation phase of translation causing a global reduction in protein synthesis.

In addition to its global effect, eIF2α phosphorylation has been shown to cause a translational up-regulation of normally repressed mRNA in yeast systems. This mRNA encodes the transcription factor GCN4 in yeast or ATF4 in metazoans, and these activate a group of genes to deal with the stress (Dever et al. 1992; Harding et al. 2000). Some of these downstream genes encode chaperones, ER enzymes, enzymes for lipid metabolism, amino acid transporters, enzymes for amino acid metabolism, and anti-oxidative stress response proteins.

Reversibility is an essential quality of regulation, and there are two known phosphatases that dephosphorylate eIF2(αP), including a constitutive CReP and a eIF2(αP)-specific GADD34. (Jousse et al. 2003, Novoa et al. 2003). It is not known whether the four known kinases and two known phosphatases are the only proteins that work together to regulate cellular levels of phosphorylated eIF2.

Role of eIF2α Phosphorylation in Health and Disease

Translational control mediated by eIF2 phosphorylation has considerable impact on cell homeostasis, and disease is a likely result when any part of that control is affected. Examples of the vast range of biological processes that are dependent on eIF2α phosphorylation by eIF2α kinases are listed here. PERK is an eIF2α kinase that responds to stress in the ER, an organelle involved in protein secretion; in humans homozygous for loss-of-function mutations of PERK, tissues of secretory nature are affected, and syndromes like diabetes mellitus and exocrine pancreatic dysfunction are seen (Delepine et al. 2000). As another example, HRI is mainly found in erythroid precursor cells in the bone marrow and responds to low levels of heme from iron deficiency by phosphorylating eIF2α and decreasing the synthesis of globin chains. This is important

because if there are excess globin chains, they will accumulate, misfold, and become proteotoxins that destroy the erythroid precursors such that red blood cells never get made, a condition called anemia (Chen 2000). In HRI knock out mice, an iron deficiency that normally leads to slightly lower red blood cell counts instead causes life-threatening anemia. Also, GCN2, activated by uncharged tRNAs, normally regulates neuronal activities, and knock out mice exhibit a defect in long-term potentiation and thus have memory deficits (Costa-Mattioli et al. 2005). However, the connection between neuronal activity and activation of GCN2 is unknown. GCN2 is also involved in the immune response; normally a tryptophan degrading enzyme is activated in specific antigen-presenting cells which send attenuating signals via GCN2 to modulate cytotoxic T cells and prevent rejection of allograft transplantations. However, this T immunomodulation was deficient in GCN2 knockout mice, and the transplants were unsuccessful (Munn et al. 2005). This is an example of how the effects of one eIF2α kinase can be so diverse depending on the cell type involved. Further, when PKR is activated by viral infection, it normally promotes apoptosis of virally infected cells to prevent cell-to-cell spread of the virus; cells lacking PKR and cells expressing a nonphosphorylatable form of eIF2α were resistant to apoptosis (Der et al. 1997, Jagus et al. 1999). Overexpression of this nonphosphorylatable form of eIF2α also promotes tumorigenesis as eIF2α phosphorylation usually checks cell proliferation (Wek 1994), while increased expression of PKR lowers cancer cell proliferation (Terada et al. 2000). Because eIF2α and its phosphorylation is crucial for regulation of a wide range of cell processes and relatively little is known of such an important control mechanism, its study has currently become more popular than ever before.

Role of eIF2α Phosphorylation in Plants

eIF2α phosphorylation is important to study beyond its involvement in health and disease in humans and other animals; for example, studies done in plants on translational control in response to stresses like viral infection or pesticide exposure have direct agricultural applications, such as improving crop yield and quality. Further, comparative studies done across the animal and plant kingdoms can reveal how the different evolutionary related groups took their related translation initiation machinery and diverged to adapt to a different lifestyle. Especially because plants are sessile, produce many of their own nutrients, and possess differentiated tissues, they may exhibit even more complex control mechanisms in response to different stresses than animals or fungi. Perhaps, new findings in how plants regulate translation can direct us to other mechanisms of control in the other kingdoms.

The study of translational control in plants is a relatively new field, and only a few, but interesting, findings have been documented. All three subunits of mammalian and yeast eIF2 are present in plant eIF2 and exhibit homology; one difference is that the eIF2α subunit is larger in plants. Though the overall process of translation initiation does not vary widely between the higher eukaryotes, evidence strongly suggests that the *control* mechanisms vary in many respects. For example, mammalian and plant eIF2 both bind to GTP or GDP via their γ subunit, but the mammalian equivalent binds GDP much more tightly relative to GTP than plant eIF2 does for the two nucleotides (Browning 1996). The K_d for rabbit reticulocyte eIF2 is 100-fold higher for GTP than that for GDP, while the K_d for wheat germ eIF2 is only 10- to 20- fold higher for GTP than for GDP. Because of plant eIF2's weak association with GTP and GDP, the

necessity of eIF2B in recycling of the nucleotides is questionable in plants, though orthologs of all five eIF2B subunits have been found in the plant genome.

This raises the question of whether eIF2α phosphorylation acts as a control mechanism in plants, and if it does, then what are the downstream effects? Mammalian eIF2α kinases can phosphorylate eIF2 isolated from plants, which suggests that the same eIF2 phosphorylation sites are present in plants. Indeed, eIF2α has been shown to be phosphorylated at Ser-51 by some of the eIF2α kinases (Gil et al. 2000); however, up to ten different isoforms of eIF2(αP) have been detected, as opposed to the single form found in mammalian and yeast systems, but the other phosphorylated sites have not been determined (Gallie et al. 1997). In addition, interestingly, up to four isoforms of phosphorylated eIF2β have been observed in wheat leaves and seeds, which are not yet reported in other organisms.

Of the four known eIF2α kinases that were previously mentioned, GCN2 is the only one that has been found in *Arabidopsis*. GCN2 in yeast is turned on in response to low amino acid levels and in turn up-regulates the expression of GCN4 which turns on other genes, like those for the enzymes of amino acid biosynthesis. In *Arabidopsis* treated with herbicide which affects amino acid biosynthesis, we see an increase in eIF2(αP) only when GCN2 is present (Zhang et al. 2008). However, the plant homologue of GCN4 has not been found, and genes that are turned on in response to the herbicide treatment are turned on even in the absence of GCN2. These findings suggest that phosphorylation of eIF2 may have different effects in plants and that the plant may not be entirely dependent on GCN2-phosphorylation of eIF2α and may rely on other regulatory mechanisms to cope with the stress when GCN2 is absent.

In addition to GCN2, PKR-like activity has been observed in wheat, but screens of the expressed sequence tag and genomic data don't reveal any PKR orthologue (Gil et al. 2000). The plant PKR-like protein responds to viral infections like mammalian PKR, resulting in eIF2α phosphorylation; however, the significant down-regulation of protein synthesis that is observed in mammalian cells is absent in plant cells, which may use other anti-viral defenses. Additionally, heat shock in plants does not induce eIF2α phosphorylation, and the response to this stress may differ considerably between plants, yeast, and animals.

Even though eIF2α phosphorylation has not been shown to be activated in plants by certain types of stresses that would otherwise induce eIF2 phosphorylation in mammalian and yeast systems, it has been shown to regulate plant development. eIF2 in embryos is found in a phosphorylated form, and in leaves, eIF2 is in a dephosphorylated form (Gallie et al. 1997); if phosphorylation actually leads to inactivation of eIF2 as it does in other organisms, then this could explain the activation of translation that occurs during germination.

There remains much to be discovered about the physiological significance of eIF2α phosphorylation in plants, which leads to the significance of this research. It is extremely beneficial, if not essential, to create mutants of eIF2α in order to study the effects on phosphorylation and regulation. This would be a dauntingly arduous task if we relied on mutations in plants, crossing them, growing them, and screening for knock-outs, so we designed recombinant protein using *de novo* synthesis of genes of all three subunits of wheat eIF2, which can later be specifically modified by insertion mutagenesis and studied biochemically. We synthesized the genes by overlapping oligonucleotides that

were optimized for *E. coli* codon usage. These genes are cloned into an operon for expression of the protein complex in *E. coli*. Obtaining large amounts of the soluble eIF2 complex from *E. coli* has been a difficult task, so the focus of this paper is on identifying optimal conditions for the expression and purification of wheat eIF2.

Methods

Cloning: synthesis of wheat eIF2 subunit genes and formation of eIF2βαγ construct

The full-length gene was synthesized for each eIF2 subunit from a set of 60 base-pair long oligonucleotides by overlap extension PCR. We used DNAWorks to reverse transcribe the wheat eIF2 subunit amino acid sequences into the corresponding DNA sequence minus intron regions and specific restriction enzyme sites (via silent mutations). More importantly, relying on the redundancy of the genetic code, the DNA sequence was optimized for expression in *E. coli* by adjusting codon bias. A Biobrick prefix and suffix consisting of specific restriction enzyme sites were added to the 5' and 3' end of the gene, respectively, for cloning purposes (**Figure 3**). The full-length genes for the three subunits of eIF2 were each cloned into separate, intermediate, non-expression vectors

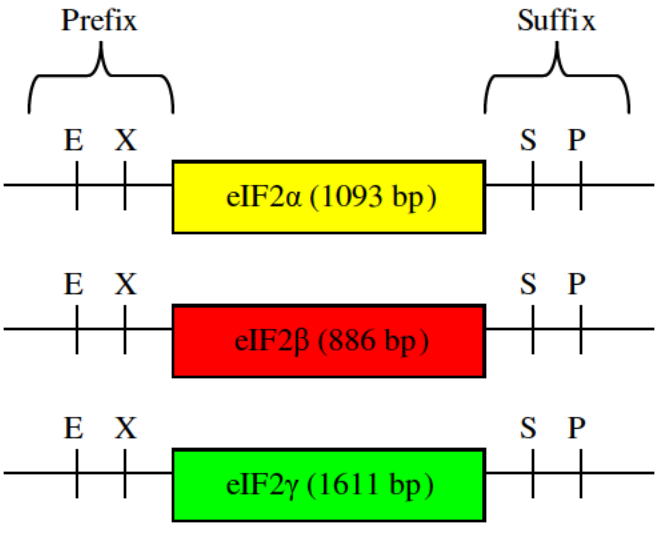

Figure 3. 5' to 3' assemblies of full-length subunit gene and Biobrick prefix and suffix containing restriction enzyme cut sites. E- EcoRI, X- XbaI, S- SpeI, P- PstI.

now called "Biobrick" vectors, and using the Biobrick construction, we can place the subunits upstream or downstream of each other in a single vector. For example, if the vector containing eIF2β gene is cut with SpeI and PstI and the vector containing eIF2α is cut with XbaI and PstI, we easily create complementary overhangs that can anneal, efficiently placing eIF2α downstream of eIF2β. We can then place eIF2γ downstream of eIF2βα without disrupting the latter pair through use of the same restriction enzymes. This is possible because upon ligation of overhangs created by XbaI and SpeI, the resulting double-strand sequence is not recognized by either enzyme (**Figure 4**). By repeating standard molecular cloning techniques, including restriction enzyme digests, ligation, transformation, and screening (all detailed later), the eIF2βαγ construct in the intermediate, non-expression vector was made.

XbaI: T/CTAGA	SpeI: A/CTAGT	Post-ligation: TCTAGT
AGATC/T	TGATC/A	AGATCA

Figure 4. Sequences recognized by restriction enzymes XbaI and SpeI. The original cut sites of the two enzymes are different in sequence at the ends, but the overhangs generated by their cutting activity are complementary and can anneal to one another. The resulting sequence on both DNA strands is recognized by neither XbaI or SpeI.

Expression of wheat eIF2βαγ operon in BL21 (DE3) cells

Cloning of the eIF2βαγ coding sequence into the pET22bb vector containing a bacteriophage T7 promoter and subsequent transformation of competent strains of *E. coli* allowed for T7 RNA polymerase-dependent expression of eIF2 protein complex. The DE3 expression host has a chromosomal copy of the T7 RNA polymerase gene under *lacUV5* control. When IPTG (Isopropyl β-D-1-thiogalactopyranoside), a mimic of allolactose, is added to the bacteria, the cells are induced because the normally repressed

T7 RNA polymerase gene is transcribed and translated, which then transcribes the eIF2 operon. The most common of the competent strains of *E. coli* used as expression hosts is BL21 (DE3), which is also useful because it is deficient in the *lon* protease and *ompT* outer membrane protease that can degrade proteins during purification. The pET22bb-eIF2 plasmid was provided by Priyanka Parekh and introduced to BL21 (DE3) cells. Two 5 ml cultures were started using a single colony in LB broth (+ 50 ug/ml ampicillin) and incubated at 37ºC with shaking at 250 rpm during the day. Both 5 ml were then used to inoculate two 50 ml fresh LB broth and were incubated overnight (16 h) at 37 ºC with shaking at 250 rpm. Both 50 ml were added to two 800 ml of fresh LB broth and OD_{600} was monitored every hour until 0.5 ± 0.1. When this OD_{600} was reached, a 1 ml uninduced culture sample was taken (pelleted, resuspended in 100 ul 1x Sample Buffer + DTT, and frozen) for SDS-PAGE analysis. Expression of eIF2 was induced by addition of 1 mM IPTG to the culture at 37ºC for 2 h. 1 ml induced culture samples were taken every hour for SDS-PAGE analysis, and the remaining cells were harvested by centrifugation for 10 min at 10,000 rpm and then frozen.

Determination of protein solubility

The pellet was subjected to freeze-thaw lysis and resuspended in 10 ml 100 mM KCl N^1 buffer (10% glycerol, 20 mM HEPES pH 7.6, 100 mM EDTA, 2 mM DTT, 7.46 g KCl per L) with 1 mini protease inhibitor tablet (Roche) until homogenous. To further disrupt cell membrane for lysis, the cells were sonicated in 5 pulses: 3 x 30 sec at 70% watt intensity and 2 x 30 sec at 90% watt intensity with 1 min cooling periods between with inversion. A rough separation of cell debris and cell lysate was done by low-speed centrifugation at 15,000 rpm for 15 min. If eIF2 is produced as inclusion bodies, or

aggregates of insoluble protein, it will be found in the pellet, so we collect a sample of it, resuspend in 100 ul 1x Sample Buffer + 2M DTT, and freeze for SDS-PAGE analysis. The supernatant was then diluted with lysis buffer (100 mM KCl N^1 buffer + protease inhibitor) to a total volume of 25 ml and subjected to high-speed centrifugation at 48,000 rpm for 45 minutes. A 40 ul sample of the high-speed supernatant was collected, mixed with 10 ul 4x Sample Buffer + DTT, and froze for SDS-PAGE analysis.

SDS-PAGE protein analysis and Western immunoblot analysis

15 ul of uninduced and induced (1 h and 2 h) samples as well as pellet and supernatant samples were heated at 95°C for 5 min and run on 12.5% SDS-PAGE gel with protein marker and eIF2 wheat germ control. The gel was stained with Coomassie Brilliant Blue for 1 h and destained overnight. The same samples are run on another 12.5% SDS-PAGE gel and transferred to PVDF membrane (Millipore Immobilon™) for 45 min at 100 mA using 25 mM Tris-base, 192 mM glycine, 20% MeOH for the transfer. The membrane is blocked in 5% milk/HNAT (10mM Hepes/KOH, pH 7.6, 150 mM NaCl, 0.2% BSA, Tween 80) for an hour at room temperature. Then the membrane is incubated overnight at 4°C in primary rabbit anti-eIF2α antibody diluted to 1:2,000 in 5% milk/HNAT. The membrane is washed several times with HNAT and incubated in the horseradish peroxidase-conjugated secondary goat anti-rabbit antibody diluted to 1:20,000 in 5% milk/HNAT for an hour at room temperature and then washed several times. The horseradish peroxidase substrate (90% SuperSignal West Pico Chemiluminescent Substrate and 10% SuperSignal West Femto Chemiluminescent Subtrate) is added and allowed to react for 5 min. The light signal is detected on Kodak film after 30 sec exposure in the dark room using Kodak GBX Developer and Fixer

solutions. The membrane is striped (5 ml 20% SDS, 2.5 ml 1.25 M Tris HCl pH 6.8, 350 ul BME, 17.5 ml diH_2O; heated for 30 min at 65 ºC) and reprobed separately with anti-eIF2β and anti-eIF2γ antibodies.

Affinity purification of antibodies from serum

The eIF2-subunit specific antibodies are affinity purified from polyclonal rabbit serum raised to wheat germ eIF2. 100 ug wheat germ eIF2 was run on SDS-PAGE gel and transferred to nitrocellulose membrane. The bands representing the eIF2 subunits were detected with fast-stain (0.025% fast green, 12% acetic acid, 50% methanol) and were each excised as strips. The stain was removed with HNAT, and the strips were blocked in HNAT for 1 hr at room temperature. Then, they are incubated in 1 ml antibody serum overnight (16 h) at 4 ºC with shaking. The strips are washed several times with HNAT to remove excess serum, transferred to a new tube, and incubated in 1 ml 0.1M glycine pH 2.2 for 10 min at room temperature to strip off the antibody. The antibody solution is then neutralized with 100 ul 1M Tris base and dialyzed against HN in 50% glycerol for 4 hr at 4 ºC to concentrate. The concentrated antibody solution is stored at -20 ºC.

Expression of wheat eIF2βαγ operon in Arctic Express (DE3) cells

Often, when *E. coli* cells are forced to express a heterologous protein and there are not enough chaperonins around to process all of the newly formed proteins, inclusion bodies, or insoluble, inactive protein aggregates, result because of the accumulation of large amounts of incorrectly folded proteins. Lowering the growth temperature to slow down the overall bacterial growth and adding chaperonins that are functional at this lower temperature may help increase the solubility of protein. An *in vivo* method of adding

chaperonins is the use of Arctic Express cells, a special strain of *E. coli* that co-express chaperonins Cpn10 and Cpn60. These proteins are from a psychrophilic bacterium *Oleispira antarctica* and are thus cold-adapted, allowing the usually mesophilic *E. coli* to grow at low temperatures.

The pET22bb-eIF2βαγ plasmid was transformed into Arctic Express (DE3) cells. Two 5 ml cultures were started using a single colony in LB broth (+ 50 ug/ml ampicillin) and incubated at 37 ℃ with shaking at 250 rpm during the day. Both 5 ml were then used to inoculate two 50 ml fresh LB broth, which was incubated overnight (16 h) at 37℃ with shaking at 250 rpm. Both 50 ml were added to two 800 ml of fresh LB broth and these cultures were incubated at 25 ℃ until OD_{600} was 0.5 ± 0.1. When this OD_{600} was reached, a 1 ml uninduced culture sample was taken (pelleted, resuspended in 100 ul 1x Sample Buffer + DTT, and frozen) for SDS-PAGE analysis. The cells were induced by addition of 1 mM IPTG and incubated at 25 ℃ for 3 h or at 10 ℃ overnight (16 h). 1 ml culture samples were taken every hour for the 3h induction and a 1 ml culture sample was taken the next day for the overnight induction, and the remaining cells were harvested by centrifugation for 10 min at 10,000 rpm and then subjected to freeze-thaw lysis. The same methods given above were followed to separate the soluble lysate (supernatant) from the insoluble pellet.

Ion exchange chromatography: phosphocellulose column

The supernatant containing the soluble protein mixture is syringe-filtered through a 0.22 um filter to remove large bacterial contaminants or passed through a Sephadex G-25 column to quickly remove low molecular weight materials. Then, the filtered supernatant is loaded onto a 5 ml phosphocellulose column previously equilibrated with

100 mM KCl N[1] buffer (10% glycerol, 20 mM HEPES pH 7.6, 100 mM EDTA, 2 mM DTT, 7.46 g KCl per L). The column is washed with 100 mM KCl N' buffer to get rid of unbound protein and eluted with 300 mM KCl N[1] buffer (same as above but 22.38 g KCl per L) to collect weakly bound proteins in 1 ml fractions, monitored by absorption at 280 nm. eIF2 from wheat germ is known to elute between 370 and 440 mM KCl, so we elute it with 500 mM KCl N[1] buffer (same as above but 37.3 g KCl per L). Absorption peak fractions are analyzed by SDS-PAGE analysis.

Cloning: formation of eIF2βγα construct

Sometimes protein expression and solubility is affected by the operon construct, so we try rearranging the order of the three subunit genes in the vector. Because the eIF2 protein complex model shows that eIF2γ has binding sites for the other two eIF2 subunits and the latter two don't have binding sites for each other, we place the eIF2γ gene between the genes for eIF2β and eIF2α, so that upon transcription and translation, eIF2γ can stabilize the other subunits as they are getting made. The eIF2β gene must be at the beginning because its Biobrick prefix is missing the XbaI cut site so it can't be placed downstream of any of the other genes. To form the eIF2βγα construct in the Biobrick non-expression vector, we repeat restriction enzyme digests, ligations, transformations, and screenings using colony PCR.

Restriction enzyme digests: 50 ul double digest reactions were made up of 3-5 ug plasmid, 5 ul appropriate 10x NEBuffer™, 0.5 ul BSA, and 2.5 ul of each NEB® enzyme (20,000 U/ul). The reactions were carried out at 37 ℃ for 4 h. The vector fragment was phosphatase-treated for 15 min at 37 ℃ to prevent re-ligation of the vector (6 µl 10x NEB® Antarctic phosphatase buffer, 1 µl 5000U/µl NEB® Antarctic phosphatase, and 3 ul

sterile diH_2O). The restriction enzymes are then inactivated at 65℃ for 20 min. All of the reactions were run on 1% agarose gel to separate the fragments. The fragments were quickly viewed under UV illumination and appropriately cut out of the gel. The DNA was recovered using Ambion spin columns and centrifugation at 3,000 rpm for 10 min.

Ligation: 10 ul ligation reactions are set up using a 3:1 molar ratio of insert to vector dependent on the sizes of the fragments, 50 ng vector fragment, 1.5 ul 10x NEB® T4 DNA ligase buffer, and 1 ul 400,000U/ul NEB® T4 DNA ligase and incubated at 16℃ overnight.

Transformation: 50 ul DH5α cells are incubated with 2 ul of the ligation reaction for 30 min, heat shocked at 42℃ for 90 seconds, and returned to ice immediately. The cells recover in 100 ul SOC broth and shake at 37℃ for 1 h. Then all of the cells are plated on LB amp plates, spread using ColiRollers plating beads, and incubated at 37℃ overnight. Note for transformation into Arctic Express cells for expression, heat shock at 42℃ for 30 s only.

Colony PCR: The colonies are screened for true positives in a 25 ul colony PCR reaction (0.5 ul 10 mM dNTPs, 5 ul 5x buffer + Mg^{2+}, 0.5 ul 25 mM MgCl, 1.25 ul 10 uM forward primer, 1.25 ul 10 uM reverse primer, 0.15 ul Taq DNA polymerase). The forward and reverse primers are oligonucleotides internal to the coding region of the subunit genes. The cycling conditions are 94℃ for 5 min, 35 repeated cycles of denaturation (94℃ for 30 sec), annealing (55℃ for 30 sec), and elongation (72℃ for 90 sec), and a final 72℃ for 5 min. The PCR reactions are run on 1% DNA agarose gel and 5 ml cultures are set up from those colonies that represent true positives. After overnight

incubation at 37℃, the cells are harvested, and the plasmids are miniprepped using GenElute™ Plasmid Miniprep Kit (Sigma-Aldrich®).

Expression of wheat eIF2βγα operon in Arctic Express (DE3) cells

The eIF2βγα coding sequence is cloned into the pET22bb vector, and after sequences are confirmed, 1 ng is transformed into Arctic Express (DE3) cells. Expression with induction at 10℃ overnight and purification on PC column with N^1 buffers of the same concentrations were done the same way aforementioned and compared with expression and purification when using the eIF2βαγ operon.

This expression was later done on a larger scale (starting with 4.8 L culture) with 2% ethanol addition to the media prior to induction, and the supernatant from the lysed cells was loaded onto a 4 ml PC column equilibrated with 300 mM KCl N^1 buffer and eluted with 500 mM KCl N^1 buffer. Then, to further purify the sample, either gradient ion exchange chromatography or size exclusion chromatography was performed.

Gradient ion exchange chromatography

The peak fractions containing proteins from the 500 mM elution are pooled and diluted with N^1 buffer (no salt) to a conductivity equivalent of 250 mM KCl. The pooled fractions were applied to a 4 ml phosphocellulose thin column previously equilibrated with 250 mM KCl N^1 buffer, and the column was eluted with a 40 ml linear gradient of 250—500 mM KCl. 1 ml fractions were collected, and every other fraction was analyzed on SDS-PAGE gel.

Size exclusion chromatography (gel filtration)

The peak fractions from the 500 mM elution are pooled and dialyzed against 100 mM KCl N^1 buffer in 50% glycerol at 4℃ overnight. A 100 ml S200 column

equilibrated with 100 mM KCl N^1 buffer was first calibrated using the Gel Filtration Standard BioRad® and washed. The concentrated pooled fractions (2 ml) were layered on this column. Based on the calibration, we can determine how many volumes must elute before proteins of the size of the eIF2 complex (molecular weight ~150,000) start eluting. Similarly, we can determine how many volumes must elute before proteins of the size of the individual non-complexed subunits (molecular weight ~50,000) start eluting. 1 ml fractions are collected and the presence of eIF2 in these fractions is confirmed using ELISA.

Enzyme-linked immunosorbent assay (ELISA)

50 ul of every other fraction (antigen) was applied to the wells and incubated overnight at 4ºC (or 30 min at room temperature). The unbound antigen was removed by aspiration and wells were washed with HNAT. Make sure to leave first well for blank (no antigen). 100 ul HNA was added to each well for blocking, incubated at room temperature for 30 min (or overnight), and then removed. Wells were washed with HNAT, and 50 ul of rabbit anti-eIF2α antibody diluted 1:2000 in HNAT (or 50 ul of rabbit polyclonal eIF2 antibody diluted 1:5000 in HNAT) was added and removed after 1 h incubation at room temperature. Wells were washed with HNAT, and 50 ul of peroxidase-conjugated goat anti-rabbit antibody diluted 1:1000 in 30% bovine serum/HNAT was added and removed after 1 h incubation at room temperature. After washing the wells with HNAT, 100 ul of the color reagent ABTS (2,2N-azino-di-3-ethylbenzthiozoline-6-sulphoric acid) was added for 15 minutes and the color reaction was stopped with 100 ul 1% SDS. The absorbance was read at 405 and 450 nm in the plate reader and adjusted for baseline absorbance determined by blank.

Growth in minimal media and ammonium sulfate precipitation

Four 5 ml Arctic Express cultures and four 50 ml in LB Broth were started and incubated with shaking overnight at 37 ℃. The cells are then pelleted at 10,000 rpm for 10 min to remove the LB broth, and the pellets are then resuspended and added to four 1 L minimal media (per liter: 8 g Na_2HPO_4, 3 g KH_2PO_4, 0.5 g NaCl, 0.5 g NH_4Cl, 3 g glucose, 2 mM $MgSO_4$, 1 mM $FeCl_3$, 0.1 mM $CaCl_2$, 100 mg ampicillin, 5 mg thiamine, 1 mg biotin, 1 mg folic acid, 1 mg niacinamide, 1 mg panthothenate, and 1 mg riboflavin) and incubated at room temperature until OD_{600} is 1.2 (by mistake); then, the cells are induced with 1 mM IPTG for 12 h at room temperature and collected by centrifugation for 10 min at 10,000 rpm. The above protocol for resuspension, lysis, and separation of soluble and insoluble fractions was followed. The supernatant (45 ml) was brought to 40% ammonium sulfate by the addition of 10.17 g $(NH_4)_2SO_4$. After stirring for 30 min, the precipitated proteins were collected by centrifugation for 15 min at 15,000 rpm. The supernatant was then brought from 40% to 70% ammonium sulfate by the addition of 8.19 g $(NH_4)_2SO_4$, and after stirring for 30 min, the precipitated proteins were collected by centrifugation for 15 min at 15,000 rpm. The pellet was dissolved in 1 ml of 100 mM KCl N^1 buffer and the resulting 4 ml was loaded onto a 120 ml S200 column equilibrated with 100 mM KCl N^1 buffer. The collected fractions were then subject to ELISA to confirm the presence of eIF2.

Results

Expression of eIF2βαγ operon in BL21 (DE3) cells

In expression studies of eIF2βαγ tricistronic construct in BL21 (DE3) cells under IPTG-dependent T7 RNA polymerase control, we looked for a detectable difference in

the expression of all three subunits in the uninduced and induced total cell extract. In theory, when the T7 RNA polymerase is fully induced, almost all of the cell's resources gets converted to expression of our target gene, such that our target protein can make up 50% of the total cell protein a few hours after induction. Based on the Coomassie stained gel, in **Figure 5(a)**, eIF2α appears to be well-expressed after 1 h of induction, as there is an obvious appearance of a 42kDa band that corresponds to the control eIF2α and was not present in the uninduced sample. Equal amounts of cell samples are loaded and the amount of expressed eIF2α seems to increase from 1 h to 2 h after induction, as expected. The expression of eIF2β and eIF2γ is not clear because the uninduced sample contains proteins of similar sizes to eIF2β and eIF2γ (38kDa and 52kDa, respectively), which may be due to leaky eIF2 expression caused by the basal expression of the T7 RNA polymerase or may simply be endogenous *E. coli* protein. Note that the eIF2γ control protein doesn't run with the 50 kDa protein marker but actually runs less. That there is no increase in expression (ie the band corresponding to the sizes of eIF2β and eIF2γ does not get darker) following induction makes it questionable whether these two subunits are actually getting expressed robustly or expressed at all.

Using affinity-purified antibodies for Western immunoblot analysis shown in **Figure 5(b)**, we confirm the expression of eIF2α post-induction as well as the absence of eIF2α expression before induction; in addition, eIF2β, thought not obvious in the Coomassie gel, is detected in the induced samples but mostly degraded. This instability may be the first evidence of no eIF2 complex formation. The expression of eIF2γ is still unclear because we don't have anti-eIF2γ antibody and instead used polyclonal anti-eIF2 antibody that picks up a lot of background. After lysing the 2 h- induced cells and

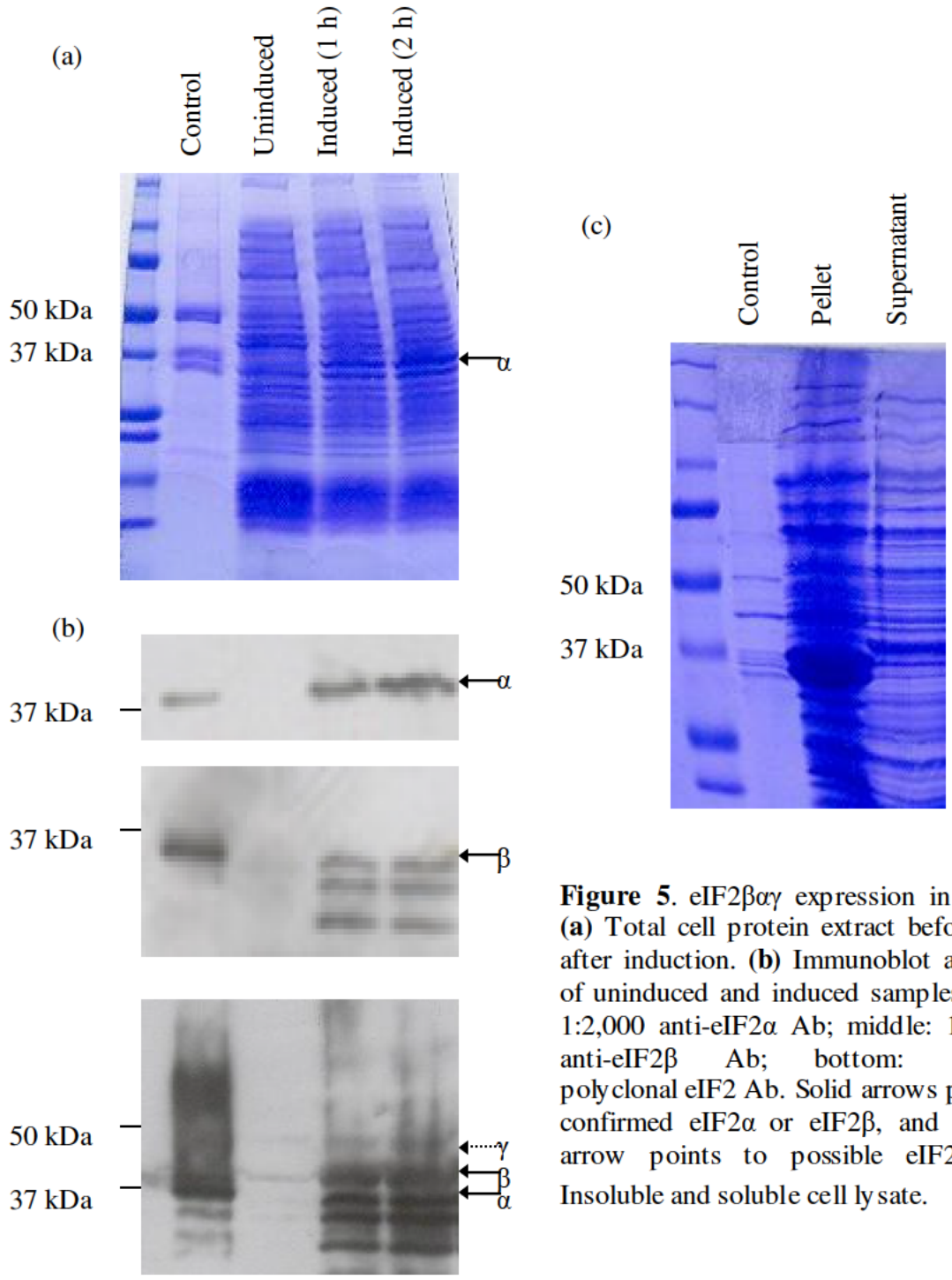

Figure 5. eIF2βαγ expression in BL21. **(a)** Total cell protein extract before and after induction. **(b)** Immunoblot analysis of uninduced and induced samples. Top: 1:2,000 anti-eIF2α Ab; middle: 1:2,000 anti-eIF2β Ab; bottom: 1:5,000 polyclonal eIF2 Ab. Solid arrows point to confirmed eIF2α or eIF2β, and dashed arrow points to possible eIF2γ. **(c)** Insoluble and soluble cell lysate.

analyzing the soluble cytoplasm and insoluble cytoplasm shown in **Figure 5(c)**, the expression of all three subunits seems promising but the majority of eIF2 is in the insoluble fraction, most likely in the form of inactive inclusion bodies. We address this

insolubility problem by expressing eIF2 in Arctic Express cells, a strain of *E. coli* that grows at lower temperatures and expresses additional chaperonins which should function in processing newly formed proteins.

Expression of eIF2βαγ operon in Arctic Express cells at 25 ºC and 10 ºC

By lowering the temperature, thereby decreasing the overall rate of protein synthesis, we hope to increase the proportion of eIF2 in soluble form. When induction occurs at 25ºC for 3 h in Arctic Express cells, expression of all three subunits is evident as shown in **Figures 6(a)**. A small amount of the eIF2 subunits is seen in the uninduced sample probably due to basal expression of T7 RNA polymerase and thus basal expression of our target protein, but nonetheless we still see an increase in expression following induction. Note that the newly affinity-purified eIF2γ antibody detects both eIF2γ and eIF2β,likely due to cross-contamination from the polyclonal serum to the eIF2 complex. At this growth and induction temperature, all of the eIF2γ produced seems to be in the insoluble fraction, although detectable amounts of eIF2α and eIF2β appear in the soluble fraction as verified by the Western blot in **Figure 6(b)**. This soluble fraction was placed on a phosphocellulose column, an ion exchange column to roughly separate the proteins and eliminate as much endogenous protein as possible. Two different concentrations of salt buffers were used to elute protein: 300 mM and 500 mM KCl N^1 buffer. It is known that the eIF2 complex from wheat germ is known to elute between 370 and 440 mM KCl. The complex is able to bind the column at higher salt concentrations than individual subunits, which elute at lower salt concentrations. Thus, if eIF2 was formed as a complex, we would see it in the 500 mM fractions; however, most of it elutes at 300 mM (not shown), so we are not getting complex formation, which

makes sense since eIF2γ is almost entirely in the insoluble fraction and thus not present to hold together the other two subunits.

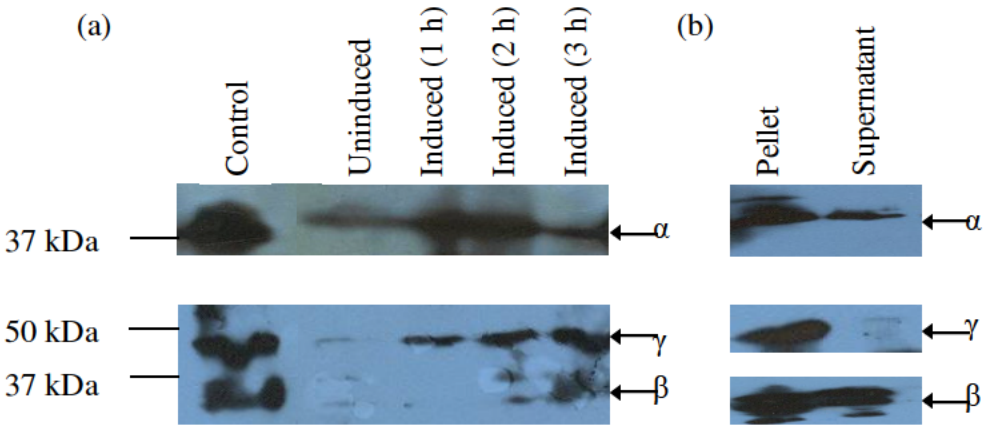

Figure 6. eIF2βαγ expression in Arctic Express cells at room temperature. **(a)** Immunoblot analysis of uninduced and induced samples. Top: 1:2,000 anti-eIF2α Ab; bottom: 1:2,000 anti-eIF2γ (also detects eIF2β). **(b)** Immunoblot analysis of insoluble and soluble cell lysate. Top: 1:2,000 anti-eIF2α Ab; middle: 1:2,000 anti-eIF2γ Ab; bottom: 1:2,000 anti-eIF2β Ab.

Thus, we try to slow growth of the cells even further in an attempt to get more soluble eIF2 complex. After 10ºC overnight induction, all three subunits expressed well and eIF2γ appears in the soluble form, along with eIF2α and eIF2β (partly degraded), as shown in **Figure 7(a)**. After running the soluble lysate on another phosphocellulose column and eluting with 300 mM and 500 mM KCl N^1 buffer (**Figure 7(b)**), one of the peak fractions (number 16 from the 500 mM elution contains all three subunits, which suggests that perhaps the complex is forming (**Figure 7(c)**). However, immunoblot analysis is a very high sensitivity test that will pick up even the slightest signal or protein, and based on the Coomassie stained gel in **Figure 7(d)**, there appears a very low amount of eIF2 complex within a pool of endogenous protein. Note that there appears to be dark

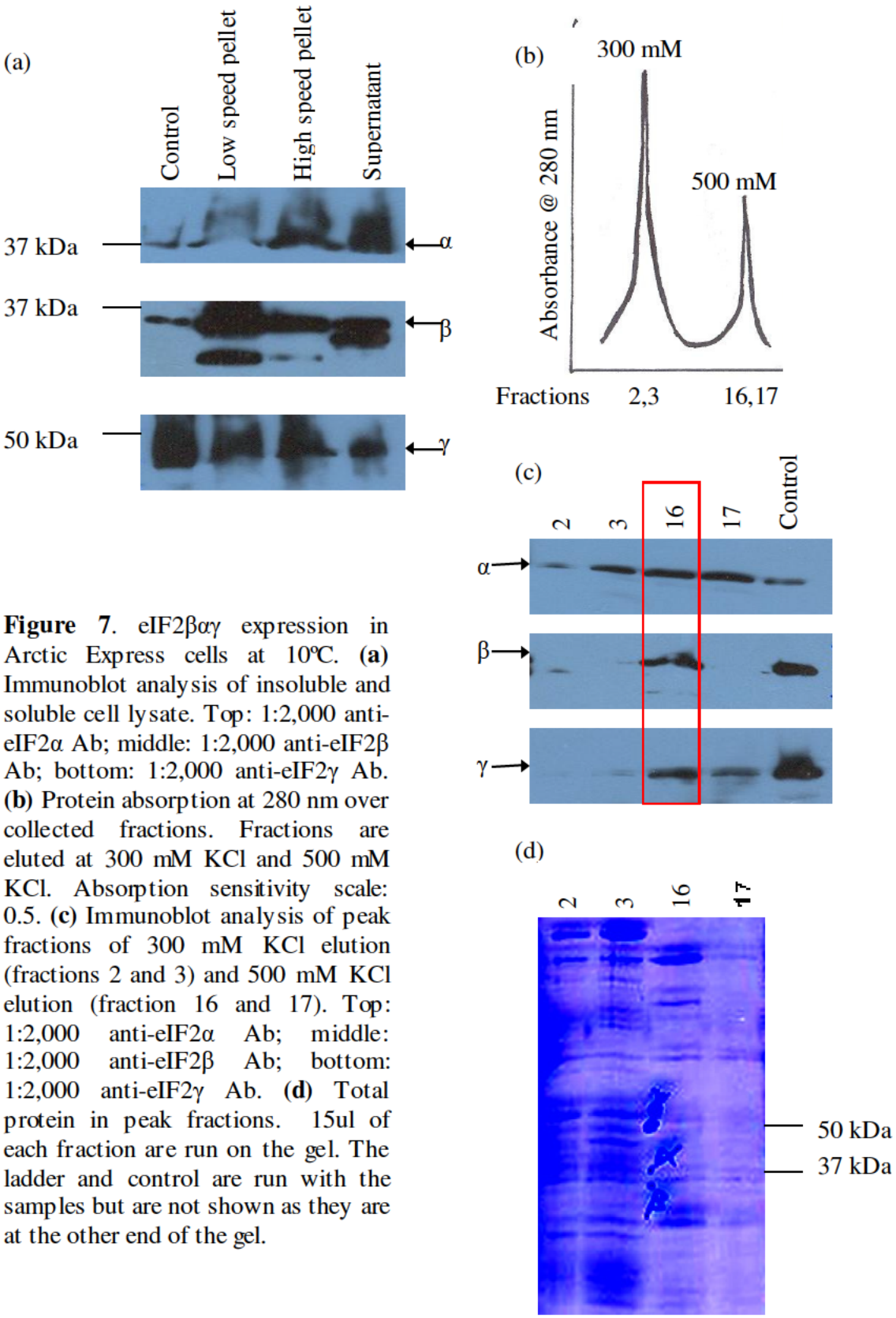

Figure 7. eIF2βαγ expression in Arctic Express cells at 10℃. **(a)** Immunoblot analysis of insoluble and soluble cell lysate. Top: 1:2,000 anti-eIF2α Ab; middle: 1:2,000 anti-eIF2β Ab; bottom: 1:2,000 anti-eIF2γ Ab. **(b)** Protein absorption at 280 nm over collected fractions. Fractions are eluted at 300 mM KCl and 500 mM KCl. Absorption sensitivity scale: 0.5. **(c)** Immunoblot analysis of peak fractions of 300 mM KCl elution (fractions 2 and 3) and 500 mM KCl elution (fraction 16 and 17). Top: 1:2,000 anti-eIF2α Ab; middle: 1:2,000 anti-eIF2β Ab; bottom: 1:2,000 anti-eIF2γ Ab. **(d)** Total protein in peak fractions. 15ul of each fraction are run on the gel. The ladder and control are run with the samples but are not shown as they are at the other end of the gel.

bands of the size of the three subunits in fractions 2 and 3 of the Coomassie stained gel, but according to immunoblot analysis, these stained proteins are not confirmed to be eIF2 subunits, except for eIF2α. Because we need to further purify the fractions containing eIF2 to eliminate contaminants and confirm that eIF2 is present in complex form, this low of an amount of eIF2 will easily get diluted during purification, and we will lose the protein. To enhance protein complex formation, we believe that rearranging the three subunit genes in the operon may be beneficial as the order of subunit formation and their subsequent interaction may contribute to the overall stability of the complex.

Formation of eIF2βγα operon and expression in Arctic Express cells at 10ºC

A view of the structure of eIF2 shows that eIF2γ binds both eIF2α and eIF2β, and the latter two don't have binding sites for each other; therefore, we place the gene for eIF2γ in between the other two genes with belief that when the protein is made, the close proximity of eIF2γ can help stabilize the other two subunits in order to form a complex. In addition, by placing the larger gene, eIF2γ, in the middle of the polycistronic construct, we increase the chance of completing its transcription before the RNA polymerase falls off the gene thereby increasing the chance of its expression. Before, when eIF2α was the middle gene, we saw that its expression was very robust, so we hope that eIF2γ will be similarly strongly expressed from this new construct.

We start from individual genes already cloned into Biobrick vectors, BB-eIF2α, BB-eIF2β, and BB-eIF2γ, where the size of the Biobrick vector is approximately 3000 bp, and the sizes of the subunits are 1093 bp, 886 bp, and 1611 bp, respectively. We first insert eIF2γ into BB-eIF2β. After restriction enzyme digests of BB-eIF2γ with XbaI

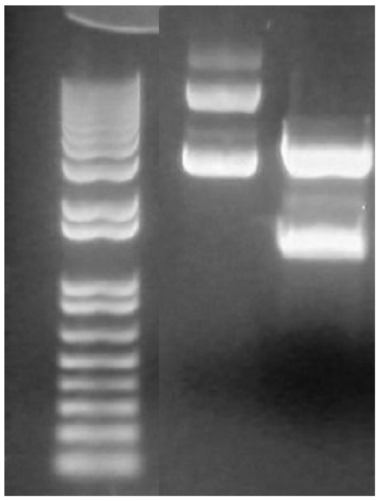

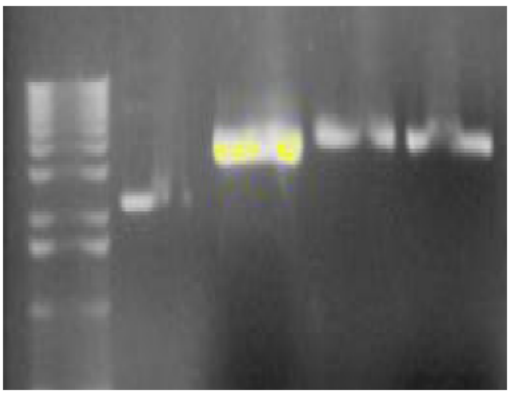

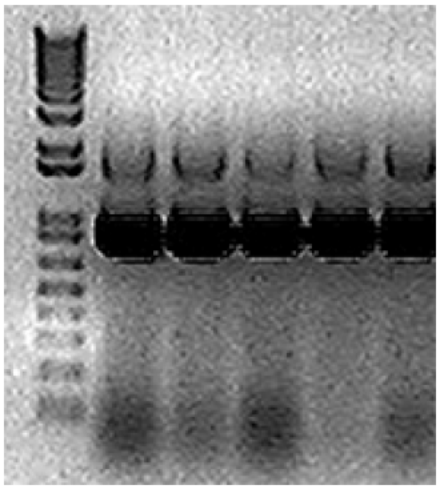

and PstI, we see in **Figure 8(a)**, as expected, one larger fragment about the size of the Biobrick vector (3000 bp) and one smaller fragment about the size of eIF2γ (1611 bp), the latter which we extract from the gel. The uncut plasmid is supercoiled and thus runs faster than linear or circular plasmids, and we can compare it with the cut plasmids to verify that our cut plasmids are indeed cut. In the double digest of BB-eIF2β with SpeI

and PstI shown in **Figure 8(b)**, we only see one fragment about 3800 bp because the shorter distance of the SpeI cut site to the PstI cut site is so small that it runs off the agarose gel; we confirm that the plasmid was linearized by running uncut, supercoiled plasmid and we check that both enzymes worked by running singly-digested plasmid. The 3800 bp fragment served as the backbone in the ligation reaction. After ligation and transformation, the presence of the correct insert was confirmed by colony PCR, using internal oligonucleotides of these two subunit genes as primers. If the eIF2γ gene did not get inserted into the BB-eIF2β backbone, we will not see any distinctive band on the gel, but if it did, then we should see a band of about 880 bp, the distance between the annealing sites of the forward and reverse primers. All tested colonies were correct as shown in **Figure 8(c)**, and we prepared a large amount of the new BB-eIF2βγ plasmid so that we can proceed to insert eIF2α into this plasmid.

BB-eIF2α was cut with XbaI and PstI and we get two bands of approximately 3000 and 1093 bp as shown in **Figure 9(a)**. BB-eIF2βγ was cut with SpeI and PstI, and in **Figure 9(b)**, we see one band of about 5500 bp, which is the backbone of the ligation reaction. To see if eIF2α was properly inserted into the BB-eIF2βγ backbone, we run a colony PCR using primers that should give us a 500 bp band for true positives; as seen in **Figure 9(c)**, all colonies tested were true positives.

To clone eIF2βγα into the pET22bb vector for expression, the eIF2βγα coding sequence was cut out of the Biobrick vector using EcoRI and PstI. Because the coding sequence and the vector are similar in size and hard to distinguish, we cut the vector with an additional enzyme, XhoI. XhoI has two cut sites on the Biobrick vector that are separated from each other by 900 bp and the XhoI cut site is separated from the EcoRI

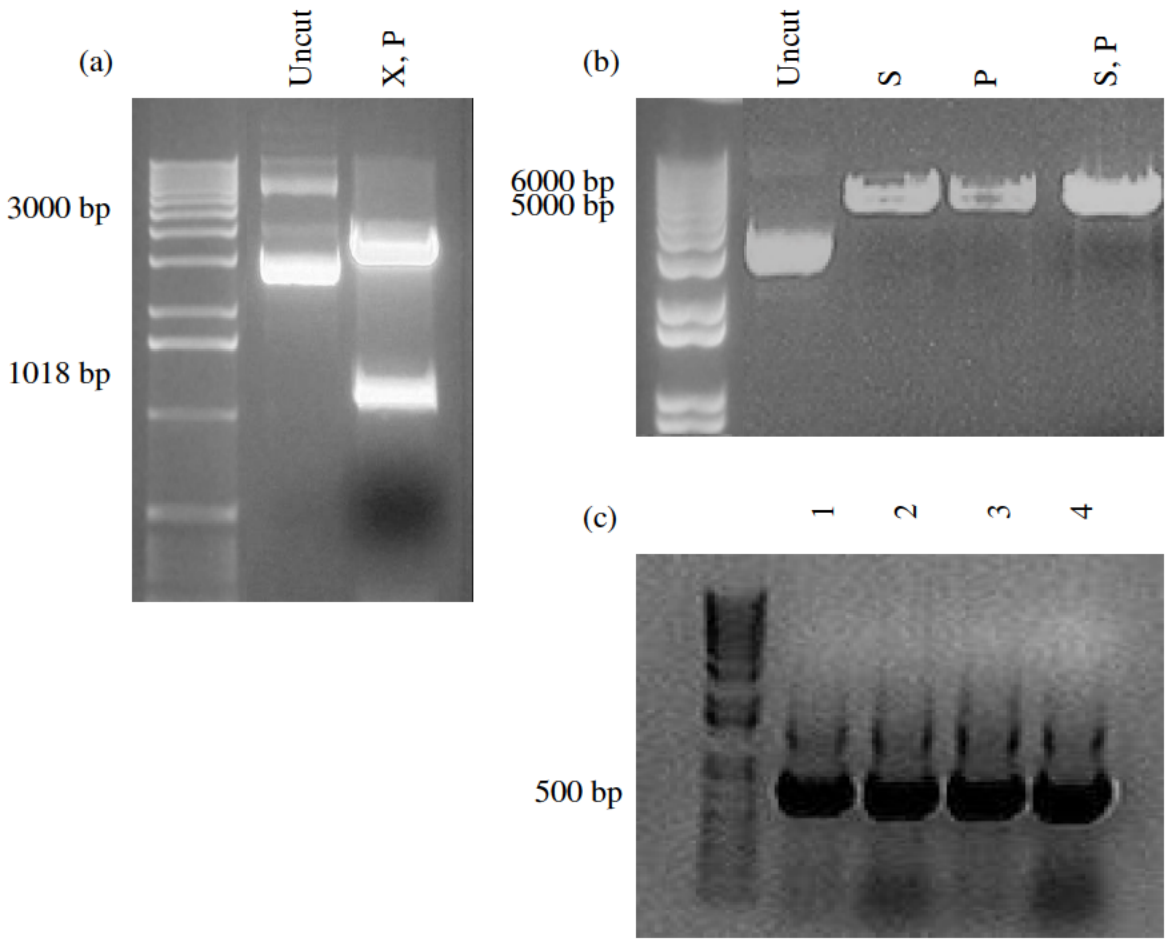

Figure 9. Cloning of BB-eIF2βγα from BB-eIF2βγ and BB-eIF2α. **(a)** Restriction enzyme digests of BB-eIF2α with XbaI and PstI. Uncut plasmid is shown for comparison. Smaller fragment is extracted. **(b)** Restriction enzyme digests of BB-eIF2βγ with SpeI and PstI. Uncut plasmid and single digests are shown for comparison. Larger, visible band is extracted. **(c)** Colony PCR screening of 4 different colonies. True positives are identified by PCR band at 500 bp.

cut site or PstI cut site by about 1000 bp. Thus after complete digestion, we should get one fragment of about 3600 bp for the coding sequence and another fragment of about 1000 bp for the chopped up backbone, as observed in **Figure 10(a)**. To test the enzymes' functionality, we also set up single digests for each of the enzymes. The previously

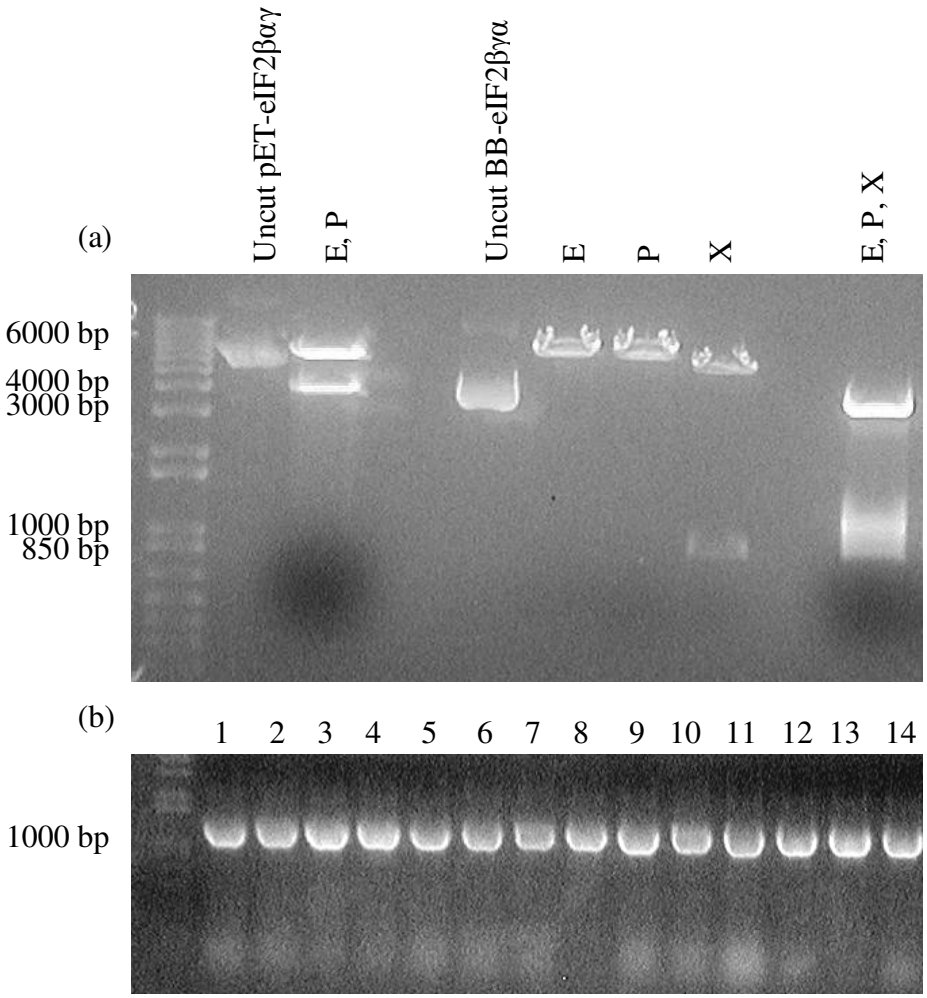

Figure 10. Cloning of pET-eIF2βγα. **(a)** Restriction enzyme digests of pET-eIF2βαγ with EcoRI and PstI. Uncut plasmid is shown for comparison. Larger fragment is extracted. **(b)** Restriction enzyme digests of BB-eIF2βγα with EcoRI, PstI, and XhoI. Uncut plasmid and single digests are shown for comparison. Larger fragment is extracted.

cloned pET22bb-eIF2βαγ vector was also cut with EcoRI and PstI, and we generate a fragment of the size of the coding sequence (3600 bp) and a fragment the size of the pET22bb backbone (5500 bp). Because we expect true positives to be 1000 bp, the colony PCR results in **Figure 10(b)** show that we successfully cloned eIF2βγα in the pET22bb vector and are ready for expression studies.

Expression of eIF2βγα operon in Arctic Express cells at 10 ºC

Keeping bacterial growth conditions the same as for expression of the eIF2βαγ operon and applying the cell soluble lysate to a PC column, we can compare the fractions collected from the expression of the eIF2βγα operon with that of the eIF2βαγ operon. The most obvious difference is that there is higher absorbance or more protein in the fractions from the 500 mM KCl elution for the new eIF2 construct, which may suggest that we are getting more stable complex formation (**Figure 11(a)**). The Coomassie stained gel in **Figure 11(b)** reflects this difference in the amount of protein, and the visible bands are of the correct size for the three subunits of eIF2. We confirm the identity of the proteins in peak fractions 14 and 15 through immunoblot analysis shown in **Figure 11(c)**. All three subunits are in these fractions. Note that the difference in relative amounts of each subunit shown in the Western blots is not real; though a look back at the Coomassie suggests that there is a difference in the relative amounts of each subunit, where eIF2γ seems to be most dominant. Even though all three subunits are copurifying after this single purification step, we must be able to show that they continue copurifying as we apply the peak fractions to other columns in order to eliminate *E. coli* contaminants.

We scale-up our starting material by growing and inducing 4.8 L of Arctic Express cells at 10 ºC. To further slow down bacterial growth, we also added 2% ethanol to the medium prior to induction, though this did not have any appreciable effect on the amount of protein produced (not shown). We confirm that eIF2 is indeed induced (not shown) and put the supernatant on a phosphocellulose column equilibrated with 300 mM KCl N^1 buffer. We then do a single elution with 500 mM KCl N^1 buffer and apply

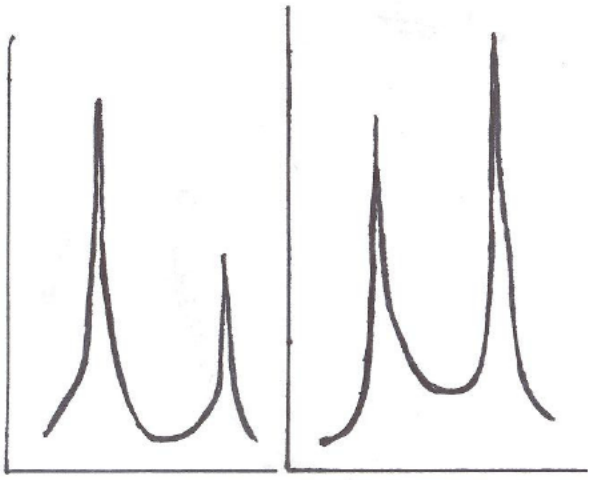

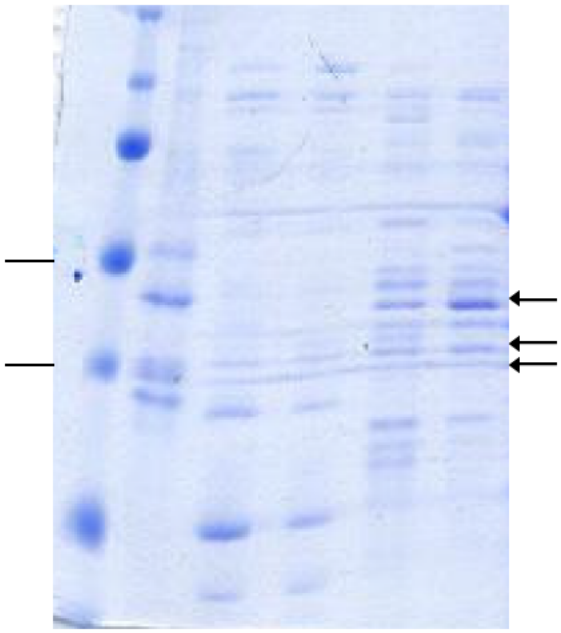

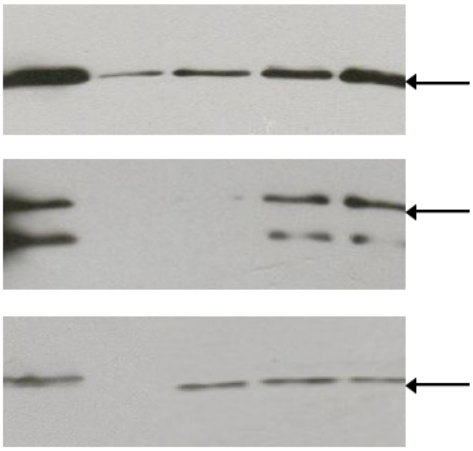

the peak fractions to another thin phosphocellulose column that we elute with a 250 mM to 500 mM KCl salt gradient to clean up the protein mixture. However, when the fractions collected were analyzed on SDS-PAGE gel, we found that we had lost eIF2γ in

the column for unknown reasons, and eIF2β and eIF2α did not copurify (ie, they were found in different fractions). This suggested that the interactions of the subunits were not strong and we did not get eIF2 complex formation.

Next, we tried size exclusion chromatography to easily distinguish between large protein complexes and smaller single subunits. In size exclusion chromatography, the larger proteins elute before the smaller proteins, so we hope for more protein coming off the column early as that suggests complex formation. The molecular weight of the eIF2 complex is close to the 158 kDa marker (which elutes at 53 ml), while the molecular weight of the individual subunits is closer to the 44 kDa marker (which elutes at 69 ml). In **Figure 12**, we can see that after 53 ml have eluted (fraction 16), where we expect the eIF2 complex to elute, there is an increase in protein absorbance at 280 nm and this increase nearly corresponds with the increase in absorbance of color at 405 and 450 nm from a strong reaction of eIF2α and its antibody (ELISA). Note that the tubing between absorbance detector and fraction collector is about 2 ml, so absorbance peaks may be off by 2 fractions (1 ml each). The assay only needs to be done with antibody to one of the subunits because if eIF2α is confirmed in the fractions where only proteins of high molecular weight are present, we can assume that the high molecular weight protein is a complex of eIF2α, eIF2β, and eIF2γ. In addition, in later fractions where the individual subunits hypothetically are, we see a weaker color absorbance and thus weaker reaction of eIF2α and its antibody, suggesting that more of it is found in the complex form. However, when we perform a Western analysis, we do not detect eIF2β or eIF2γ in any of the fractions where the complex should be so it may be that we never got complex formation and that the large proteins containing eIF2α may actually be aggregates of

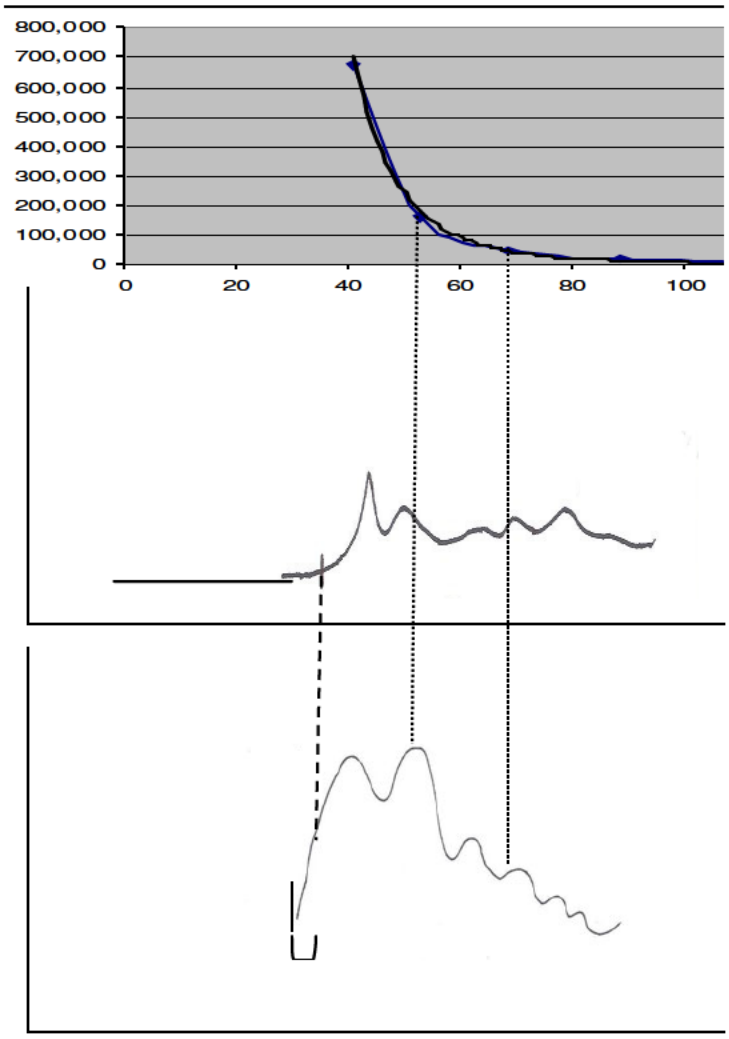

Fraction	A_{405}	A_{450}
2	0.462	0.109
4	0.962	0.170
6	1.265	0.214
8	1.417	0.231
10	1.459	0.235
12	1.242	0.205
14	1.108	0.194
16	1.324	0.219
18	1.520	0.248
20	1.527	0.263
22	0.903	0.164
24	0.671	0.137
26	0.809	0.151
28	0.737	0.146
30	0.592	0.122
32	0.485	0.102
34	0.568	0.119
36	0.550	0.123
38	0.319	0.090
40	0.367	0.092
42	0.187	0.062
44	0.232	0.070
46	0.058	0.043
48	0.089	0.059
50	0.173	0.059

eIF2α, so we must go back to target expression conditions. In addition, we do not detect any eIF2β or eIF2γ in any of the fractions where the individual subunits should be, so they may have been diluted during gel filtration, and again we must alter our expression conditions to optimize the protein yield. It may also be that the low salt concentration of the buffer was not optimal for the complex and caused disassociation of what might have been a complex.

Growth of Arctic Express cells in minimal media and purification by ammonium sulfate precipitation and size exclusion chromatography

Bacterial growth is hampered by growing the cells in minimal media such that they can't rely on the surrounding nutrients in the media to readily supply them with building blocks and energy. They only receive the bare minimum, like a carbon source (glucose), nitrogen source (NH_4Cl), and various salts to synthesize on their own the amino acids and nucleic acids that they need. By placing this stress on the bacteria, theoretically they should waste less of their nutrients and energy to support growth and instead devote the majority of their supplies to the formation of our targeted protein after induction.

We try this method of growth and then perform an ammonium sulfate precipitation to roughly purify proteins based on their solubility in ammonium sulfate. Using this method, we can quickly remove contaminants as well as concentrate our target protein for subsequent loading on a S200 column. Wheat germ eIF2 is known to precipitate out of solution in the 40-70% ammonium sulfate range, so assuming that recombinant eIF2 behaves similarly, we collect the insoluble fraction from the 40-70% ammonium sulfate fractions, resuspend it, and subject it to the next step of purification.

Following gel filtration with a 120 ml S200 column equilibrated with 150 mM KCl N[1] buffer (salt concentration higher than previously) and ELISA using polyclonal eIF2 antibodies, we determined that none of the fractions contain any subunit of eIF2. Results from this series of steps are inconclusive, and if allowed more time, gels would be run to determine 1) whether eIF2 was expressed when cells were grown in minimal media, 2) whether eIF2 was found in the soluble or insoluble cell cytoplasm, 3) whether eIF2 was found in the 40-70% or 0-40% ammonium sulfate precipitate fraction, and 4) whether the antibody dilution was too high for the ELISA.

Discussion and Future Direction

Although we were unsuccessful at purifying soluble recombinant eIF2 from *E. coli* cells, the failed experiments provide us with some insight and direction for future work. First, comparison of eIF2 expression in BL21 and Arctic Express cells suggests that the latter are more suitable for increasing solubility of eIF2α and eIF2β. The coexpression of chaperonins in Arctic Express cells may improve solubility of the eIF2 subunits by ensuring the correct folding of these proteins. Next, the solubility of the more cumbersome eIF2γ in Arctic Express cells was achieved by lowering the induction temperature from room temperature to 10ºC, the optimal temperature at which these chaperonins function. Although overall growth and eIF2 production is compromised, it is more important, to a certain extent, to obtain soluble proteins in lower concentrations than an excess of incorrectly folded, insoluble proteins that are difficult to recover in its active form through *in vitro* techniques. (Of course, the most optimal result is still to have a large amount of soluble protein). We may want to slow down our target protein expression and enhance solubility even further by lowering IPTG concentrations or by

transforming and expressing eIF2 in Novagen Tuner cells. These are BL21 cells that lack the *lac* permease so that IPTG uniformly enters all the cells in the culture and we can precisely control the level of induction in a concentration-dependent manner. The expression of eIF2 in Tuner cells can be then compared with that in Arctic Express cells.

In previous literature, it has been shown that the soluble expression of recombinant proteins in *E. coli* often depends on the medium composition. When growing bacteria in minimal media versus rich LB broth, we again slow overall growth to enhance solubility of our protein. Whether this worked in our experiment is inconclusive but for future studies, an analysis of the effectiveness of growing cells in minimal media would be useful. Trace metals were omitted from the media in this experiment and may have an inhibiting effect on metabolic processes and protein formation, so in future studies, trace metals may be necessary. The growth of cells in minimal media, though slow, needs to be carefully monitored to ensure that the cells are in healthy condition when they are induced. If cells are already at stationary phase working hard just to survive, chances are that they won't work very hard to produce undesired foreign proteins like our target protein and may in fact stimulate plasmid instability. Other media composition alterations including supplementation with 1% glucose prior to induction to decrease the amount of T7 RNA polymerase by catabolite repression so that we can regulate transcription and expression of our target protein. Even though this may slow down growth, it may not necessarily have any appreciable positive effect on the expression of our protein, as observed in the case with addition of 2% ethanol to the media, or it may also over-down-regulate our protein expression, so it is important to determine optimal conditions for bacterial expression of our recombinant protein.

Successful expression of multifactorial proteins is not only based on solubility but also on whether the protein complex is formed with the correct subunit interactions. Whether complex formation occurs can be determined if the subunits copurify in successive purification steps. To enhance protein complex formation, first, we cloned the three subunits genes into an operon under control of one promoter so that they are transcribed and translated at the same time and place; then, we tested different gene arrangements or constructs. The eIF2βαγ and eIF2βγα constructs were separately expressed, and purification of the proteins from the latter construct seemed more promising—there was more protein in the 500 mM KCl elution, where we expect eIF2 complex to come off the column, than in the 300 mM KCl elution, suggesting that there may be more complex formation. One explanation might be that the closer proximity of the eIF2γ gene to eIF2α and eIF2β genes in the eIF2βγα operon leads to ribosome processing of polycistronic mRNA in sequential order such that the formation of the large eIF2γ, which holds together the complex in native eIF2 models, before formation of both of the other subunits contributes to stable complex formation. Due to this speculation, we completely abandoned the eIF2βαγ construct for expression, but it may be useful to reexamine and optimize expression from this operon construct as well. In addition, other arrangements can be tried, especially one where eIF2γ gene is placed at the beginning of the operon. However, this requires the manipulation of the eIF2β plasmid, which is currently missing a XbaI cut site in the prefix that prevents us from being able to place it downstream of any other gene. If complex formation still does not occur, we may have to coexpress other proteins to mimic what is naturally found in cells; however, determination of cofactors may be extremely difficult.

If we can get expression to work optimally, then the next step is to determine what series of purification methods results in the largest removal of *E. coli* contaminants and the largest recovery of eIF2. We have used two columns—PC and S200—and also tried ammonium sulfate precipitation. We can only make generalizations at this point about these purification techniques because we can't confirm that we had sufficient eIF2 complex expressed in the first place. PC columns with single salt buffer elutions are effective at removing a lot of bacterial contaminants but surely aren't sufficient. When gradient salt buffer elutions are conducted on PC columns, the targeted protein is diluted too far and we lose it. The same effect is also seen in size exclusion chromatography. Thus, it is important to start with a concentrated sample so that dilutions, which are inevitable, won't completely lead to the loss of our target protein. We tried to concentrate our sample through ammonium sulfate precipitation, but results are inconclusive. Future studies should be done to determine how much ammonium sulfate is necessary for precipitation of our protein and exclusion of contaminants.

After purification, there still remains the question of whether the recombinant protein is functional, which can be answered by assaying the purified protein. One assay can be done by incrementally adding recombinant eIF2 to wheat germ extracts depleted of eIF2 and measuring any restored translation activity. We can also determine if recombinant eIF2 is capable of forming the ternary complex and how strongly it binds to GTP/GDP and Met-tRNA$_i^{Met}$.

Upon confirming similar functionality of recombinant and native eIF2, we can finally take eIF2α kinases from other organisms and determine if phosphorylation of plant recombinant eIF2 occurs and whether the downstream regulatory effects are similar

to those observed in mammalian and yeast systems. Site-directed mutagenesis experiments on eIF2α can be easily conducted by changing the nucleotide sequences on the gene plasmid and expressing and purifying mutant forms of eIF2. However, the hurdle to study translation regulation in plants remains because we have not optimized expression and purification of recombinant eIF2.

Acknowledgements

Special thanks to Dr. Karen Browning, Dr. Grace Choy, and Laura Mayberry for mentoring and teaching me all the laboratory skills and Priyanka Parekh for providing the eIF2 coding plasmids.

Bibliography

Alone P.V. and Dever T.E. 2006. Direct binding of translation initiation factor eIF2γ-G domain to its GTPase-activating and GDP-GTP exchange factors eIF5 and eFI2B. *J. Biol Chem*. **281**:12636-12644.

Alone P.V., Cao C., and Dever T.E. 2008. Translation initiation factor 2γ mutant alters start codon selection independent of Met-tRNA binding. *Mol. Cel. Biol*. **28**: 6877-6888.

Asano K., Krishnamoorthy T., Phan L., Pavitt G.D., and Hinnebusch A.G. 1999. Conserved bipartite motifs in yeast eIF5 and eIF2B, GTPase-activating and GDP-GTP exchange factors in translation initiation, mediate binding to their common substrate eIF2. *EMBO J.* **18**: 1673-1688.

Bertolotti A., Zhang Y., Hendershot L.M., Harding H.P., and Ron D. 2000. Dynamic interaction of BiP and ER stress transducers in the unfolded-protein response. *Nat. Cell Biol.* **2**: 326-332.

Browning, K.S. 1996. The plant translation apparatus. *Plant Mol. Biol*. **32:** 107-144.

Buttgereit F. and Brand M.D. 1995. A hierarchy of ATP-consuming processes in mammalian cells. *Biochem. J.* **312:** 163-167.

Chen J, 2000. Heme-regulated eIF2α kinase. In *Translational control of gene expression* 1st ed., pp. 529-546. Cold Spring Harbor Laboratory Press. Cold Spring Harbor. New York.

Costa-Mattioli M., Gobert D., Harding H.P., Herdy B., Azzi M., Bruno M., Ben Mamou C., Marcinkiewicz E., Yoshida M., Imataka H., et al. 2005. Translational control of hippocampal synaptic plasticity and memory by an eFI2 kinase, GCN2. *Nature* **436**: 1166-1173.

Delepine M., Nicolino M., Barrett T., Golamaully M., Lathrop G.M., and Julier C. 2000. EIF2AK3, encoding translation initiation factor 2-alpha kinase 3, is mutated in patients with Wilcott-Rallison syndrome. *Nat. Genet*. **25:** 406-409.

Der S.D., Yang Y.L., Weissmann C., and Williams B.R.G. 1997. A double-stranded RNA-activated protein kinase-dependent pathway mediating stress-induced apoptosis. *Proc. Natl. Acad. Sci*. **94**: 3279-3283.

Dever T.E., Feng L., Wek R.C., Cigan A.M., Donahue T.F., and Hinnebusch A.G. 1992. Phosphorylation of initiation factor 2 alpha by protein kinase GCN2 mediates gene-specific translational control of GCN4 in yeast. *Cell* **68:** 585-596.

Donahue T.F., Cigan A.M., Pabich E.K., and Valavicius B.C. 1988. Mutations at a Zn(II) finger motif in the yeast eIF2β gene alter ribosomal start-site selection during the scanning process. *Cell* **54**: 621-632.

Gallie D.R., Le H., Caldwell C., Tanguay R.L., Hoang N.X., and Browning K.S. 1997.

The phosphorylation state of translation initiation factors is regulated developmentally and following heat shock in wheat. *J. Biol. Chem*. **272:** 1046-1053.

Gebauer F. and Hentze M.W. 2004. Molecular mechanisms of translational control. N*ature Rev. Mol. Cell Biol***. 5**:827-835.

Gil J. Esteban M., and Roth D. 2000. In vivo regulation of protein synthesis by phosphorylation of the alpha subunit of wheat eukaryotic initiation factor 2. *Biochemistry* **39**: 7521-7530.

Harding H., Novoa I., Zhang Y., Zeng H., Wek R.C., Schapira M., and Ron D. 2000. Regulated translation initiation controls stress-induced gene expression in mammalian cells. *Mol. Cell* **6:** 1099-1108.

Hinnebusch A.G. 2005. Translational regulation of GCN4 and the general amino acid control of yeast. *Annu. Rev. Microbiol*. **59**: 407-450.

Ito T., Marintchev A., and Wagner G. 2004. Solution structure of human initiation factor eIF2α reveals homology to the elongation factor eEF1B. *Structure* **12**: 1693-1704.

Jagus R., Joshi B., and Barber G.N. 1999. PKR, apoptosis, and cancer. *Int. J. Biochem. Cell Biol*. **31**: 123-138.

Jousse C., Oyadomari S., Novoa I., Lu P.D., Zhang Y., Harding H.P., and Ron D. 2003. Inhibition of a constitutive translation initiation factor 2α phosphatase, CReP, promotes survival of stressed cells. *J. Cell. Biol*. **163**: 767-775.

Kapp L.D. and Lorsch J.R. 2004. GTP-dependent recognition of the methionine moiety on initiator tRNA by translation factor eIF2. *J. Mol. Biol*. **335**: 923-936.

Kozak M. 1991. Structural features in eukaryotic mRNAs that modulate the initiation of

translation. *J. Biol. Chem*. **266**: 19867-19870.

Lu L., Han A.P., and Chen J.J. 2001. Translation initiation control by heme-regulated eukaryotic initiation factor 2alpha kinase in erythroid cells under cytoplasmic stresses. *Mol. Cell. Biol*. **21**: 7971-7980.

Munn D.H., Sharma M.D., Baban B., Harding H.P., Zhang Y., Ron D., and Mellor A.L. 2005. GCN2 kinase in T cells mediates proliferative arrest and anergy induction in response to indoleamine 2,3-dioxyegnase. *Immunity* **22**: 633-642.

Nanduri S., Rahman F., Williams B.R., and Qin J. 2000. A dynamically tuned double-stranded RNA binding mechanism for the activation of antiviral kinase PKR. *EMBO J.* **19**: 5567-5574.

Novoa I., Zhang Y., Zeng H., Jungreis R., Harding H.P., and Ron D. 2003. Stress-nduced gene expression requires programmed recovery from translational repression. *EMBO J.* **22:** 1180-1187.

Pestova T.V., Lorsch J.R., Hellen C.U.T. 2007 The mechanism of translation initiation in eukaryotes. In *Translational Control in Biology and Medicine*. 2nd ed., pp 92-95. Cold Spring Harbor Laboratory Press, Cold Spring Harbor. New York.

Pisarev A.V., Kolupaeva V.G., Pisareva V.p., Merrick W.C., Hellen C.U.T., and Pestova T.V. 2006. Specific functional interactions of nucleotides at key -3 and +4 positions flanking the initiation codon with components of the mammalian 48S translation initiation complex. *Genes Dev*. **20:** 4624-3636.

Rowlands, A.G., Panniers R., Henshaw E.C. 1988. The catalytic mechanism of guanine nucleotide exchange factor action and competitive inhibition by phosphorylated initiation factor 2. *J. Biol. Chem*. **263**: 5526-5533.

Terada T., Maeta H., Endo K., and Ohta T. 2000. Protein expression of double-stranded RNA-activated protein kinase in thyroid carcinomas. *Hum. Pathol.* **31**: 817-821.

Unbehaun A., Borukhov S.I., Hellen C.U.T., and Pestova T.V. 2004. Release of initiation factors from 48S complexes during ribosomal subunit joining and the link between establishment of codon-anticodon base –pairing and hydrolysis of eIF2-bound GTP. *Genes Dev*. **18**: 3078-3093.

Walden W.E., Godefroy-Colburn T., and Thach R.E. 1981. The role of mRNA competition in regulating translation. I. Demonstration of competition *in vivo*. *J. Biol. Chem.* **256:** 11739-11746.

Wek R.C. 1994. eIF2 kinases: Regulators of general and gene-specific translation initiation . *Trends Biochem. Sci.* **19**: 491-496.

Wek R.C., Jiang H.Y., and Anthony T.G. 2006. Coping with stress: eIF2 kinases and translational control. *Biochemical Society Transactions*. **34**: 1.

Yatime L., Mechulam Y., Blanquet S., and Schmitt E. 2006. Structural switch of the γ subunit in an archael aIF2αγ heterodimer. *Structure* **14:** 119-128.

Yatime L., Schmitt E., Blanquet S., and Mechulam Y. 2004. Functional molecular mapping of archaeal translation initiation factor 2. *J. Biol. Chem***. 279**: 15984-15993.

Zhang Y., Wang Y., Kanyuka K., Parry M.A.J., Powers S.J., and Halford N.G. 2008. GCN2-dependent phosphorylation of eukaryotic translation initiation factor-2α in Arabidopsis. *J. Exp. Botany* **59:** 3131-3141